Three Dimensional Micro/Nano-structure Fabrication of Phase-change Film

Y. Lin[1,3], M. H. Hong[1,2*], L. S. Tan[1], C. S. Lim[3,4], L. P. Shi[2] and T. C. Chong[1,2]

[1]*Department of Electrical and Computer Engineering, National University of Singapore, 1 Engineering Drive 3, Singapore 117576*
[2] *Data Storage Institute, DSI Building, 5 Engineering Drive 1, Singapore 117608*
[3] *Nanoscience & Nanotechnology Initiative, National University of Singapore, 2 Engineering Drive 3, Singapore 117576*
[4] *Department of Mechanical Engineering, National University of Singapore, 2 Engineering Drive 3, Singapore 117576*
**Email:* Hong_Minghui@dsi.a-star.edu.sg

Laser-crystallized features were produced on as-deposited amorphous phase-change films by laser irradiation through a microlens array, which is a highly efficient patterning method since arbitrary features can be created uniformly over a large area in a short time. An Nd:YAG laser and a femtosecond laser were used as light sources. The dependence of feature size on laser wavelength and laser dose was studied. By using the femtosecond laser, sub-100 nm features can be produced. The patterned phase-change films included 30 nm thick $Ge_1Sb_2Te_4$, $Ge_2Sb_2Te_5$, Sb_2Te_3, and GeTe films, at 30 nm thick. It was found that the amorphous and laser-crystallized phase states of different phase-change films had different reactions to alkaline solution. Three dimensional micro/nano-structures, such as holes and bumps, in phase-change films were fabricated.

DOI: 10.2961/jlmn.2008.01.0010

Keywords: laser-crystallized, phase-change film, femtosecond laser, Nd:YAG laser, microlens array, chemical etching

1. Introduction

Phase-change materials have been attracting more attention because of their unique optical and electrical properties. The phase-change materials have two phase states: amorphous and crystalline. Their different reflectivities allow phase-change materials to be applied extensively in optical data storage [1-3] and nonvolatile memory [4-6] for their unique optical and electrical properties respectively. The two phase states of phase-change materials can be converted to each other easily by laser heating. Around 140°C is need for GeSbTe films to change from the amorphous to the crystalline phase state, while around 623°C is required for it to reverse back to the amorphous state through melting and quenching processes. Different kinds of laser systems, such as the Nd:YAG laser and the femtosecond laser, were used as light sources to irradiate the as-deposited amorphous phase-change films for laser crystallization.

In this article, high-speed large-area nanopatterning of phase-change films through a microlens array (MLA) was introduced. A high-throughput and low-cost nanopatterning method, which allows complete freedom in fabricating nano-patterns, is the target of nanolithography techniques. Electron-beam nanolithography, ion-beam nanolithography, x-ray nanolithography, and near-field scanning probe nanolithography have been developed for such purposes [7-12], but they face the challenges of low throughput and high cost. Nanoimprinting lithography has attracted significant attentions recently for its high throughput [13], but it is easy to contaminate the expensive stamps used for contact patterning, which increases processing cost. The MLA patterning technique is similar to nanoimprinting technology, but it is a non-contact method, which is the advantage of optical patterning methods. MLA nanolithography has been demonstrated to pattern micro/nano-structures in polymer uniformly over a large area in a short time [14, 15]. The microlenses (same size and focal length in micron-order) in a MLA convert a laser beam into thousands of focal points, which act as an array of light "pens" to fabricate many tiny structures uniformly over a large area at a high speed.

The MLA patterning method was used to laser-crystallize phase-change films to fabricate nanofeatures uniformly over a large area in a short time. The patterned phase-change films were GeSbTe ($Ge_1Sb_2Te_4$&$Ge_2Sb_2Te_5$), Sb_2Te_3, and GeTe films. The dependence of feature size on laser dose and wavelength was studied. Making use of chemical etching, the 2D nanofeatures on the phase-change films were developed to form 3D nanostructures.

2. Experimental

Phase-change thin films, GeSbTe, Sb_2Te_3, and GeTe films, were coated on 0.6 mm polycarbonate substrates by a Balzers Cube sputtering system. The system has three independent process chambers and three sputtering power sources (two DCs and one RF). The phase change thin films were sputtered by DC magnetron sputtering methods. The distance between the target and substrate was 4 cm. The chamber background pressure was set at 1.2×10^{-7} mbar. The prepared phase-change thin films were

not annealed and were in the amorphous phase state initially.

Figure 1 shows the optical image of a MLA and the schematic diagram of the experimental setup. The number of lenses, which are made of fused silica, is 401×401 in an area of 10×10 mm^2. The diameter of each lens is 23 μm and the lenses are arranged in a hexagonal array with a pitch of 25 μm. The sag of each lens is 9 μm in height, which is equivalent to a focal length of 28.7 μm, thus giving a numerical aperture (NA) of 0.59. Different models of Nd:YAG laser: BMI 5000 (pulse repetition rate 10 Hz, pulse duration 7 ns) with fundamental and second harmonic generation at wavelengths of 1064 nm and 532 nm, respectively; Lightwave laser (Series 210G, wavelength 532 nm, pulse repetition rate 1 kHz, pulse duration 40 ns); AVIA laser (wavelength 355 nm, pulse repetition rate 1 kHz, pulse duration 100 ns), and a femtosecond laser (Spectra-physics, wavelength of 800 nm, pulse duration of 100 fs, pulse repetition rate of 80 MHz, and linearly polarized), were used to irradiate the samples through the MLA at different laser doses. The laser dose is one important parameter in photoresist exposure, which is dependent on laser fluence and pulse number applied on photoresist. The features on the phase-change films were characterized by electrical force microscopy (EFM, DI 3100, Veeco) and near-field scanning optical microscopy (NSOM, Aurora-2, Veeco) in the transmission mode.

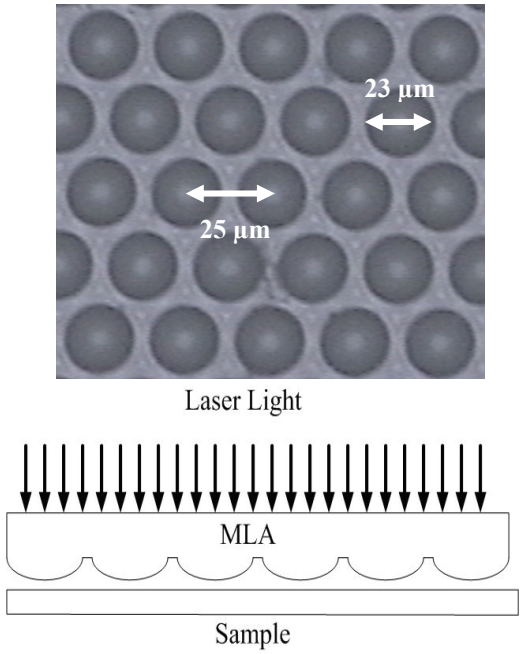

Fig. 1 Optical image of a microlens array (MLA) and schematic diagram of the experimental setup.

3. Results and discussion

3.1 Features fabricated by different lasers

3.1.1 Nanosecond laser

Different models of Nd:YAG lasers were used to irradiate the phase-change films through the MLA to study the effects of laser dose and wavelength on the pattern size. Initially amorphous phase-change films were crystallized by laser irradiation. For each wavelength of the Nd:YAG laser systems, different laser doses were tested for the laser nanopatterning. Since the transition temperature of phase-change films from the amorphous to crystalline phase state is around 140 ^{o}C, the incident laser dose was controlled to avoid ablating the phase-change films to form holes.

Figure 2 shows the dependence of the laser-crystallized feature size in the GeSbTe film on the incident laser fluence of the BMI Nd:YAG laser (wavelength 532 nm) with single pulse of the laser irradiation. It shows that the feature size increases with laser fluence almost linearly. This was also observed when different wavelengths of the Nd:YAG laser systems, such as BMI laser with 1064 nm, Lightwave laser with 532 nm, and AVIA laser with 355 nm, were used. Meanwhile, it is observed that the feature sizes obtained increase with the wavelength, which is similar to the dependence of focal spot size on wavelength. However, the smallest feature sizes fabricated are much smaller than the calculated minimum focal spot sizes, which are 1690 nm and 845 nm for the wavelengths of 1064 nm and 532 nm, respectively. For 1064 nm wavelength, the minimum experimental feature size is only around one third of the calculated focal spot size. For 532 nm and 355 nm wavelengths, the minimum fabricated feature sizes are around 40% of the calculated minimum focal spot size. This comparison suggests that the feature size can be smaller than the minimum focal spot size. The conversion of two phase states is produced by the heat treatment. Laser irradiation is used to heat the phase-change films to reach the phase change critical temperature. The affected area can be smaller than the focal spot size of the lens by controlling the incident laser dose at a sufficiently low level such that only the peak power at the center of the beam heats the phase-change films to the critical transition temperature.

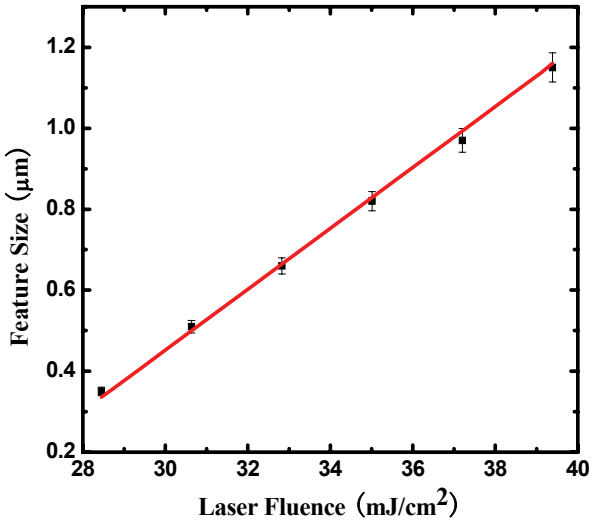

Fig. 2 Dependence of feature size on the GeSbTe film incident laser fluence under 532 nm Nd:YAG laser irradiation through a MLA.

3.1.2 Femtosecond laser

Although the minimum feature size defined by nanosecond laser irradiation is smaller than the minimum focal spot size, it cannot break through the optical diffraction limit of λ/2 by using this MLA. It was found that by mak-

ing use of a MLA with 1 μm diameter lenses, λ/3 feature size can be achieved on photoresist by excimer laser irradiation (248 nm, 23 ns) [16], but it is difficult to get such high resolution by utilizing the MLA with 23 μm diameter lenses (Fig. 1) and nanosecond laser irradiation. Therefore, a femtosecond laser was used to study the possibility of breaking the optical diffraction limit by using this MLA.

The ultrashort pulse duration of the femtosecond laser is capable of producing different phenomena from the nanosecond lasers. Figure 3 shows the dependence of feature size on the number of pulses of femtosecond laser irradiation. The dot features were fabricated by the femtosecond laser with 60, 70, 80, 90, and 100 pulses, respectively. The laser power applied was 200 mW. The average feature sizes are 400, 680, 890, 1080, and 1220 nm, respectively. Since the laser dose absorbed by the phase-change films is related to the number of pulses of laser irradiation applied, the feature size is observed to increase nonlinearly with the laser dose. The high peak intensity and short pulse duration of the femtosecond laser leads to the nonlinear effect. Many interesting nonlinear phenomena have been observed with the femtosecond laser pulses, such as supercontinuum radiation, the third-harmonic generation as the pulse duration is in femtosecond scale, and electrical conductivity of plasma channels [17-22]. Therefore, nonlinear absorption induced by high-power femtosecond laser pulses makes the feature size on the phase-change films increase nonlinearly.

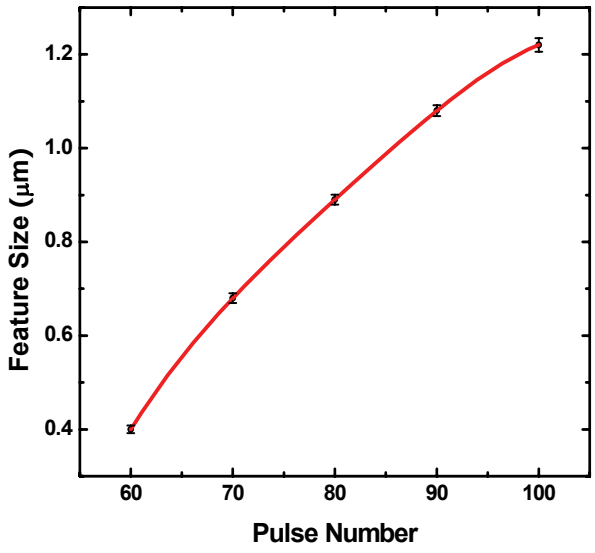

Fig. 3 Dependence of feature size on a phase-change film on the number of pulses of femtosecond laser irradiation at a laser power of 200 mW.

3.2 2D micro/nanofeatures produced by femtosecond laser

Since the optical and electrical properties of the two phase states of phase-change films are different, optical microscopy, near-field scanning optical microscopy (NSOM) and electrical force microscopy (EFM) were used to characterize the laser-crystallized features on phase-change films.

Figure 4 shows 3D EFM images of single dot features in the accompanying optical images. The ring structures can be observed clearly in the EFM images. The features were fabricated on phase-change films with the femtosecond laser at a laser power of 140 mW with 100 pulses irradiation at different MLA-to-sample distances. The rings observed are due to the diffraction effect of each lens in the MLA at the non-focal planes. Similar to atomic force microscopy (AFM), EFM uses a metal-coated probe to measure conductivity. By applying a voltage of 5 V on the patterned phase-change films, the conductive probe detected different electrical forces from the laser-crystallized and amorphous phases due to their different resistivities. The amorphous phase state has a higher resistivity than crystalline state. The "phase" signal with unit in degree in EFM is the cantilever amplitude signal, which is proportional to the electrical force and resistivity as well.

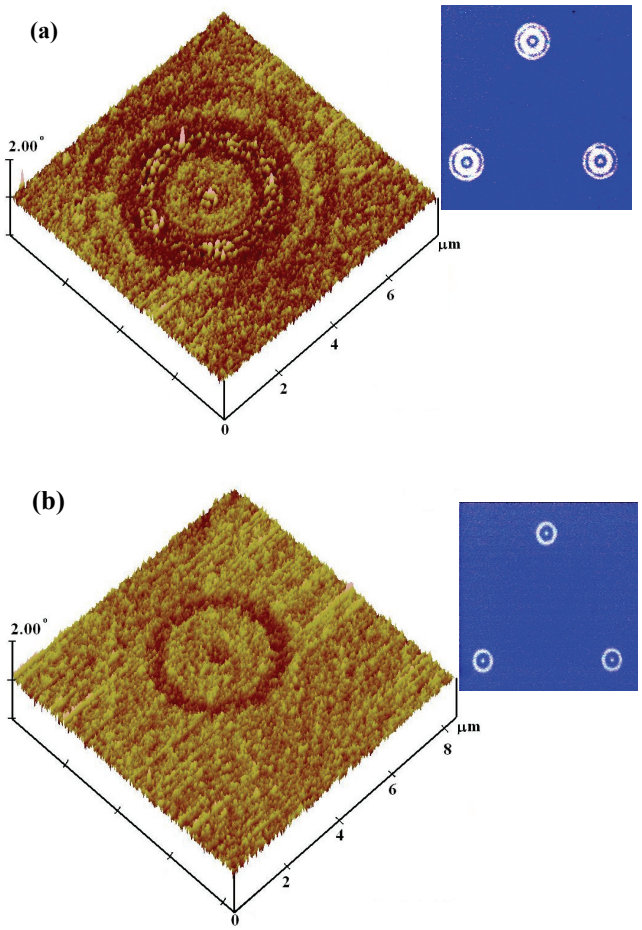

Fig. 4 3D EFM images of dot patterns on the phase-change thin films fabricated by the femtosecond laser irradiation through the MLA at an incident laser power of 140 mW and different MLA-to-sample distances.

Figure 5 shows (a) 3D transmission NSOM image and (b) 3D topography image of an array of laser-crystallized dot features in the GeSbTe films. The crystalline features on the phase-change films were fabricated by femtosecond laser with 100 pulses irradiation through the MLA at a laser power of 200 mW. The dot features in Fig. 5 were fabricated by moving the nano-stage (Model: ALS130-100-LTAS-NC, Aerotech), on which the phase-change films

were placed, at a step of 1 μm along *x* and *y* axes. The lower PMT output (in voltage unit, dark color) in the transmission NSOM image in Fig. 5(a) means that the laser-crystallized phase features have lower light transmitivity than the amorphous phase state. The topography image shows that there is no morphology change but only phase change on the patterned phase-change films.

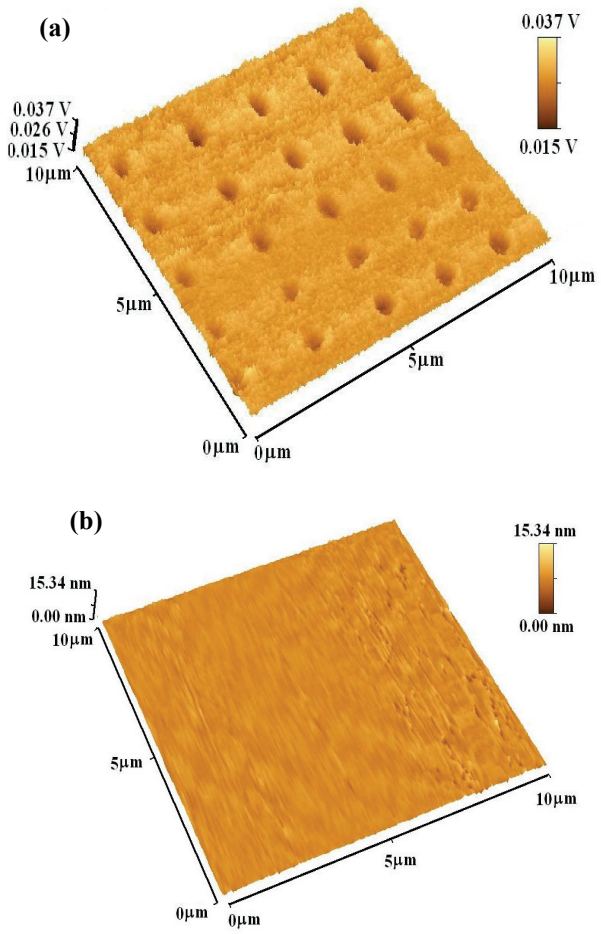

Fig. 5 (a) 3D transmission NSOM image and (b) 3D topography image of crystalline dot features in the GeSbTe films produced by the femtosecond laser with 100 pulses irradiation through a MLA at a laser power of 200 mW.

3.3 3D phase-change lithography by chemical etching

In this section, the patterned phase-change films were etched by an alkaline solution to form 3D structures. It was found that the amorphous and laser-crystallized phase states have different reactions; meanwhile the phase-change materials with different elements have different reactions to the alkaline etching solutions as well. The effects of chemical etching on GeSbTe, GeTe and SbTe films are described in the following sections. The alkaline solutions used were KOH and NaOH solutions with 30% weight concentration. It was found that these two solutions have the same effect on different phase-change films.

3.3.1 GST films

Figure 6 shows 3D AFM images of (a) bump-arrays with a period of 1 μm patterned by the femtosecond laser with 70 pulses of the laser irradiation by placing the GeSbTe film at the focal plane and (b) ring-wall features patterned with 90 pulses of the femtosecond laser irradiation by placing the GeSbTe film at the non-focal plane at a laser power of 200 mW. Both of the patterned phase-change films were dipped into a 30% alkaline solution for around 1 min. The heights of features in Figs. 6 are both around 30 nm, which is equal to the thickness of the sputtered GeSbTe films. This means that the amorphous phase state of the GeSbTe films has been etched away completely, while the laser-crystallized features were left to form 3D structures.

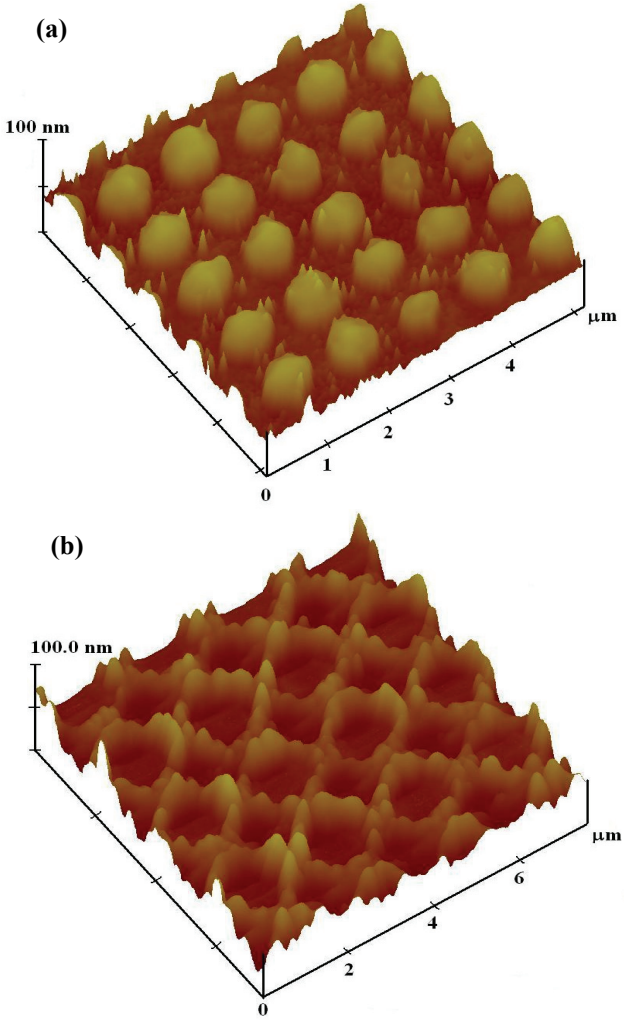

Fig. 6 3D AFM images of (a) pillar-arrays with a period of 1 μm patterned with 70 pulses of the femtosecond laser irradiation by placing the GeSbTe film at the focal plane and (b) ring-wall features patterned with 90 pulses of the femtosecond laser irradiation by placing the film at the non-focal plane at a laser power of 200 mW.

Making use of a lower laser power and fewer pulses of the laser irradiation, sub-100 nm feature size was obtained on the GeSbTe film. Figure 7 shows the line profile of a bump feature with a size of 95 nm, a full width at half maximum (FWHM) of 55 nm, and a height of 17 nm. It was fabricated at a laser power of 80 mW with 50 pulses of

the laser irradiation with the GeSbTe film subsequently dipped into a 30% alkaline solution for 1 minute.

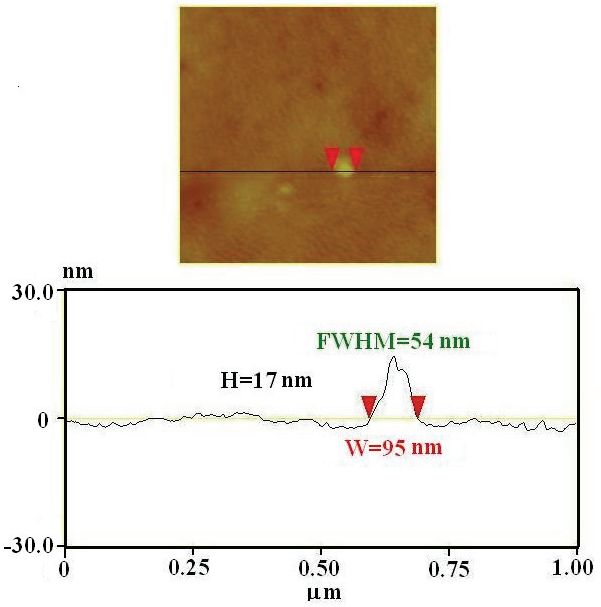

Fig.7 Line profile of a bump feature with a size of 95 nm and a full width at half maximum (FWHM) of 55 nm, and a height of 17 nm. It was fabricated at a laser power of 80 mW with 50 pulses of the laser irradiation with the GeSbTe film subsequently dipped into a 30% alkaline solution for 1 minute.

3.3.2 SbTe films

It was found that the SbTe film had a different reaction to alkaline solutions from the GeSbTe film. Figure 8(a) is a topography image of a SbTe film patterned with the femtosecond laser at a laser power of 200 mW with 50 pulses of the laser irradiation and then etched by a 30% alkaline solution for 30 seconds. For the SbTe film, it was the laser-crystallized features that were etched away in the alkaline solution. Holes instead of bumps were obtained in the film with full-width-at-half-maximum (FWHM) of around 160 nm and depth of around 46 nm. The average roughness of the film in the amorphous phase state area after the etching was around 15.4 nm measured over an area of 20 × 20 μm^2. It was found that for a longer etching time, the roughness increased greatly and the depth of the holes decreased, which implies that both the laser-crystallized features and the amorphous background were etched by the alkaline solution.

3.3.3 GeTe films

Patterned GeTe films were dipped into the same alkaline solution and it was found that the laser-crystallized features were etched away, similar to the SbTe films. Figure 8(b) is a 3D AFM image of a GeTe film patterned with the femtosecond laser at a laser power of 200 mW with 100 pulses of the laser irradiation and then etched by a 30% alkaline solution for 30 seconds. The average FWHM of the holes is 460 nm and the depth is 21 nm in average. The roughness measured is only 1.5 nm over a 20 × 20 μm^2 area in the amorphous phase state, and it increases much more slowly than the roughness of etched SbTe films.

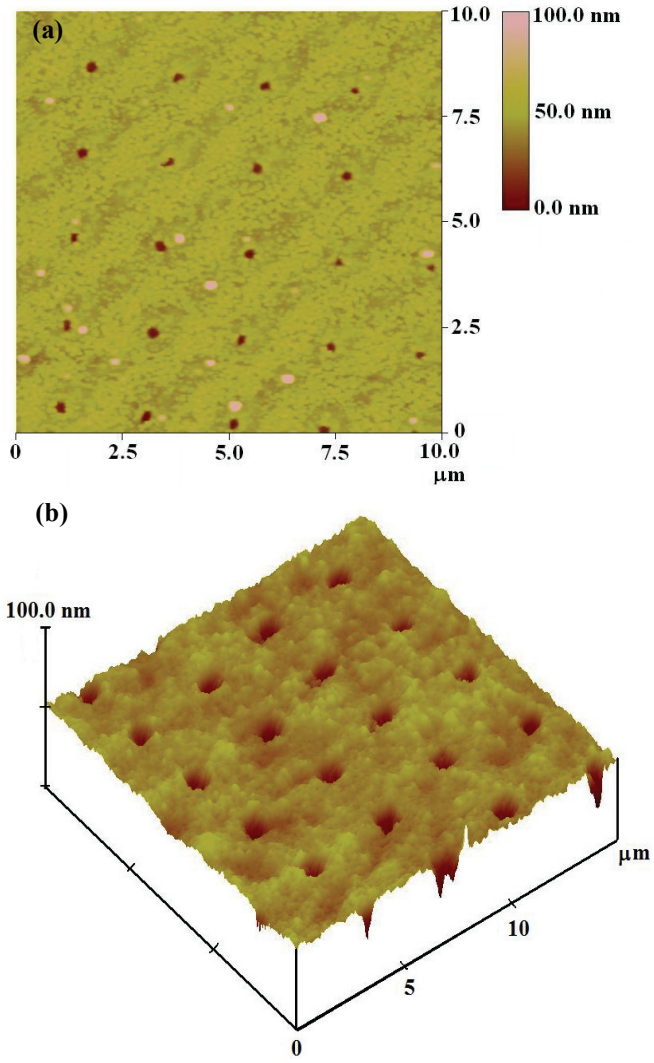

Fig. 8 (a) 2D AFM image of SbTe film and (b) 3D AFM image of GeTe film patterned with a femtosecond laser at a laser power of 200 mW with 50 pulses and 100 pulses of the laser irradiation, respectively. The films were then etched by 30% alkaline solution for 30 seconds.

3.3.4 Possible mechanisms

It was found that the three kinds of phase-change films reacted to the alkaline solutions differently for their different compositions. The amorphous background of GeSbTe films were etched away to form bumps. However, it was the laser-crystallized features of SbTe and GeTe films that were etched away, while the amorphous phase state is remained to form holes. At the same time, the roughness of the GeTe film was much lower than that of the SbTe film. Although the mechanism of the reactions of phase-change films to the alkaline solutions is not very clear, it seems that the alkaline solutions act as a catalyst in these reactions and the Ge component plays an important role in these different reactions. It is supposed that the Ge component is most inert to the alkaline solutions in Ge, Sb, and Te components since the roughness of the GeTe film is much lower than that of the SbTe film. The mechanism behind the opposite reactions of GeSbTe films to GeTe and SbTe films is still under investigation.

4. Conclusions

In this paper, the MLA non-contact patterning technique on the phase-change films with Nd:YAG lasers and femtosecond laser was demonstrated. The dependence of feature size on the laser dose and wavelength was studied. The feature size increases with the laser dose and wavelength when nano-second lasers were utilized to define patterns on the phase-change films. To overcome the optical diffraction limit and further reduce the feature size, femtosecond laser was applied. Due to the ultra-high peak power and ultra-short pulse duration of femtosecond laser, sub-100 nm feature size was obtained on phase-change films. Making use of different reactions of the two phase states of the phase-change films to the alkaline solutions, 3D phase-change lithography was demonstrated. Bumps and holes structures were fabricated in the phase-change films after etching in the alkaline solutions. In conclusion, 3D micro/nano-structures can be fabricated by laser irradiation through MLA and chemical etching over a large area with high efficiency.

Acknowledgments and Appendixes

This work is supported by the Agency for Science, Technology and Research (A*Star) in Singapore.

References

[1]. Ovshinsky, S.R.: Phys. Rev. Lett., 21, (1968) 1450.
[2]. Ovshinsky, S.R. and H. Fritzche: Metallurgical Transactions, 2, (1971) 641.
[3]. Ovshinsky, S.R. and P.H. Klose: J. Non-Cryst. Solids, 8-10, (1972) 892.
[4]. Pirovano, A., A.L. Lacaita, D. Merlani, A. Benvenuti, F. Pellizzer, and R. Bez: IEEE, (2002).
[5].Kim, Y.-T., Y.-N. Hwang, K.-H. Lee, S.-H. Lee, C.-W. Jeong, S.-j. Ahn, F. Yeung, G.-H. Koh, H.-S. Jeong, W.-Y. Chung, T.-K. Kim, Y.-K. Park, K.-N. Kim, and J.-T. Kong: Jap. J. Appl. Phys., 44, (2005) 2701.
[6]. Lankhorst, M.H.R., B.W.S.M.M. Ketelaars, and R.A.M. Wolters: Nature Mater., 4, (2005) 347.
[7]. Broers, A.N., J.M. Harper, and W.W. Molzen: Appl. Phy. Lett., 33, (1978) 392.
[8]. Flanders, D.: Appl. Phy. Lett., 36, (1980) 93.
[9]. McCord, M.A. and R.F.P. Pease: J. Vac. Sci. Technol. B, 4, (1986) 86.
[10]. Albrecht, T.R., M.M. Dovek, C.A. Lang, P. Grüter, C.F. Quate, S.W.J. Kuan, C.W. Frank, and R.F.P. Pease: J. Appl. Phys., 64, (1988) 1178.
[11]. Early, K., M.L. Schattenburg, and H.I. Smith: Microelectron. Eng., 11, (1990) 317.
[12]. Lyding, J.W., T.C. Shen, J.S. Hubacek, J.R. Tucker, and G.C. Abelin: Appl. Phy. Lett., 64, (1994) 2010.
[13]. Chou, S.Y., P.R. Krauss, and P.J. Renstrom: Appl. Phy. Lett., 67, (1995) 3114.
[14]. Wu, M.H., K.E. Paul, and G.M. Whitesides: Appl. Opt., 41, (2002) 2575.
[15]. Kato, J., N. Takeyasu, Y. Adachi, H.B. Sun, and S. Kawata: Appl. Phy. Lett., 86, (2005) 044102.
[16]. Lim, C.S., M.H. Hong, Y. Lin, Q. Xie, A.S. Kumar, M. Rahman, and S.Z. Lee: Appl. Phy. Lett., 89, (2006) 191125.
[17]. Kasparian, J., R. Sauerbery, D. Mondelain, S. Niedermeier, J. Yu, J.-P. Wolf, Y.-B. André, M. Franco, B. Prade, S. Tzortzakis, A. Mysyrowicz, M. Rodriguez, H. Wille, and L. Wöste: Opt. Lett., 25, (2000) 1397.
[18]. Aközbek, N., A. Iwasaki, A. Becker, M. Scalora, S.L. Chin, and C.M. Bowden: Phys. Rev. Lett., 89, (2002) 143901.
[19]. Yang, H., J. Zhang, L.Z. Zhao, Y.J. Li, H. Teng, Y.T. Li, Z.H. Wang, Z.L. Chen, Z.Y. Wei, J.X. Ma, W. Yu, and Z.M. Sheng: Phys. Rev. E, 67, (2003) 015401.
[20]. Hao, Z.Q., J. Zhang, Z. Zhang, T.T. Xi, Z.Y. Zheng, X.H. Yuan, and Z.H. Wang: Acta Phys. Sin., 54, (2005) 3173.
[21]. Schillinger, H. and R. Sauerbrey: Appl. Phys. B., 68, (1999) 753.
[22]. Tzortzakis, S., M.A. Franco, Y.-B. André, A. Chiron, B. Lamouroux, B.S. Prade, and A. Mysyrowicz: Phys. Rev. E, 60, (1999) R3505.

(Received: April 24, 2007, Accepted: December 16, 2007)